Heavy mesons photoproduction at distinct collision geometries in LHC

M. B. Gay Ducati
Institute of Physics, UFRGS, Brazil

Latin American Symposium
on High Energy Physics (SILAFAE)

Mexico, November, 4-8/2024

Outlook

- Theoretical Framework
  - → QCD: LE + NLE
  - → The Exclusive Photoproduction
  - → The Colour Dipole Models
- Phenomenology
  - → Ultraperipheral Collisions (UPC)
  - → Peripheral Collisions
  - → NLO study in pQCD
- Simulations
  - → Simulations with FoCal
- Summary and a Look Ahead

QCD factorization

→ Hadronic interactions

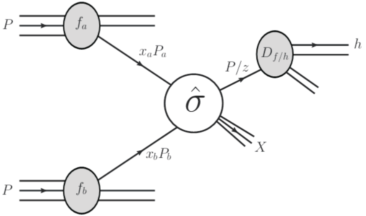

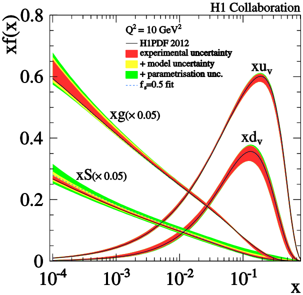

- The production cross section can be written as

$$\sigma_{hh\to hx} \propto f_{a/h}(x_1, Q^2) \otimes f_{b/h}(x_2, Q^2) \otimes \hat{\sigma}(ab \to cd) \otimes D_{h/c}(z_c, \hat{Q}^2)$$

$f_p(x, Q^2)$ → Parton Distribution Functions (PDF's): CTEQ, MRST, GRV, ...

$\hat{\sigma}(ab \to cd)$ → partonic subprocess $ab \to cd$: $qq \to qq$, $q\bar{q} \to gg$, $gg \to gg$, ...

$D_{h/c}(z_c, \hat{Q}^2)$ → fragmentations functions of hadron h from a parton c.

Saturation Phenomena

- Some evolution equations:
- Linear equations
  - DGLAP
  - BFKL
- Non-Linear equations
  - AGL
  - JIMWLK
  - BK

$x \rightarrow$ longitudinal momentum fraction
$Q^2 \rightarrow$ transferred momentum

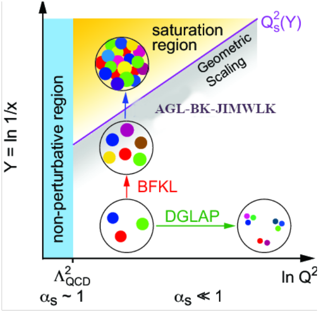

- In small-x, the gluon recombination process is important

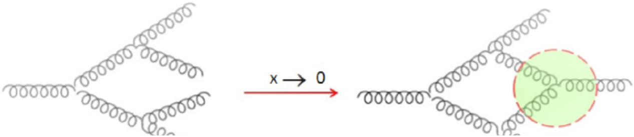

Color Dipole Formalism

Theory
The QCD Factorization
Dipole Model
Diffractive Production
W.W. Method
$\gamma - p$ Interaction
$\gamma - A$ Interaction
Dipole Cross Section
Phenomenology
Simulations
Summary

The Balitsky-Kovchegov Equation

$$\partial_Y \langle T(x,z)\rangle = \frac{\bar{\alpha}}{2\pi}\int d^2z \mathscr{M}(x,y,z)[\langle T(x,z)\rangle + \langle T(z,y)\rangle - \langle T(x,y)\rangle - \langle T(x,z)\rangle\langle T(z,y)\rangle]$$

- This equation evolves $\langle T(x,y)\rangle$ where $T(x,y)$ is the dipole realizations.
- The evolution variable is the rapidity $Y \approx \ln 1/x$.
- $\bar{\alpha}_s = \alpha_s N_c/\pi$ and $\mathscr{M}(x,y,z) = \frac{(x-y)^2}{(x-z)^2(z-y)^2}$.
- The photon splitting in the $q\bar{q}$ pair with z and $1-z$ fraction of light cone momentum.
- The quark or antiquark can emit soft gluons ($z_2 \ll z_1$), which can also emit softer gluons.
- In the limit $N_c \to \infty$, these soft gluons can be considered as quark-antiquark pairs.

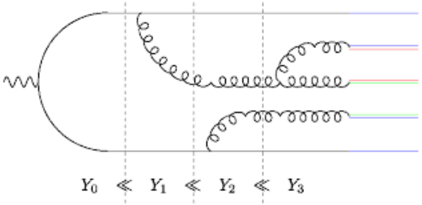

Dipole Meson Process

- Complementary information on gluons distribution can be obtained

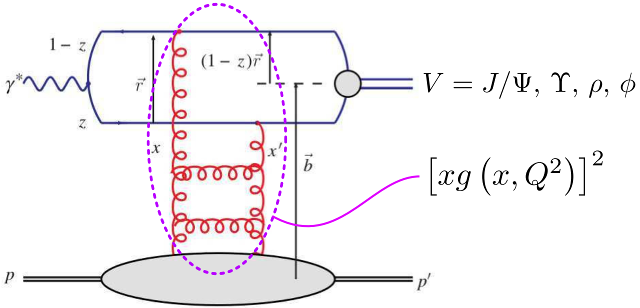

r is the dipole separation.
z(1-z) is the quark(antiquark) momentum fraction.
b is the dipole-target impact parameter.

Photo-Induced Interactions

- Diffractive production of vector mesons in hadron-hadron collisions.
- The process is characterized by large rapidity gaps in the final state.

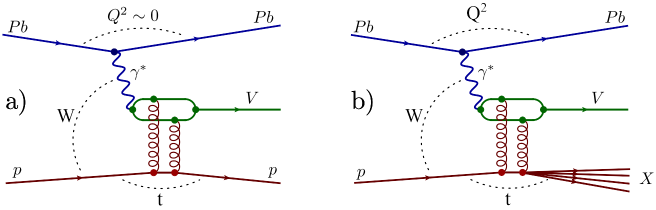

$Q^2 \rightarrow$ photon virtuality.
$W^2 \rightarrow \gamma * p$ center of mass energy.
$t \rightarrow$ squared momentum transfer.

- We are interested in the first case: **Exclusive Photoproduction ($Q^2 \sim 0$),**

$$p \otimes Pb \rightarrow Pb \otimes V \otimes p$$

Photon Flux

- **Weizsäcker-Williams Method**
- Hadron-Hadron interaction $\longrightarrow$ photon-hadron interaction

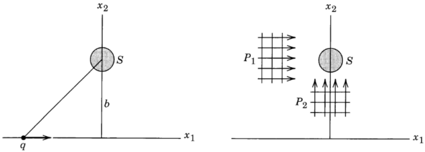

- Thus, the hadron process can be written in a simpler way

$$\sigma_X = \frac{dN(\omega)}{d\omega} \otimes {\sigma_x}^{\gamma}(\omega)$$

where the equivalent photon flux is written as

$$\frac{dI(\omega)}{d\omega} = \frac{2q^2}{\pi}\left[\chi_{min} K_0(\chi_{min}) K_1(\chi_{min}) - \frac{1}{2}\chi_{min}^2 \left[K_1^2(\chi_{min}) - K_0^2(\chi_{min})\right]\right]$$

The Photoproduction Cross Section

- For $\gamma - p$ interaction, the forward scattering amplitude is given by

$$\mathrm{Im}\, A_{\text{proton}}(x, t=0) = \int\int \frac{d^2 r dz}{4\pi} \left(\psi_V^* \psi_\gamma\right)_T \sigma_{\text{dip}}^{\text{proton}}(x, r)$$

  - $\left(\psi_V^* \psi_\gamma\right)_T$ - photon-meson wave function $\rightarrow$ Boosted Gaussian;
  - $\sigma_{dip}^{proton}(x, r)$ - dipole cross section $\rightarrow$ GBW and CGC models;;

- Then, the photoproduction cross section will be

$$\sigma\left(\gamma p \rightarrow V p\right) \propto \left|\mathrm{Im}\, A_{\text{proton}}(x, t=0)\right|^2$$

  - $x = \left(M_V^2 + Q^2\right) / \left(Q^2 + 2\omega\sqrt{s_{NN}}\right)$

The Photoproduction Cross Section

- For $\gamma - A$ interaction, the forward scattering amplitude is given by

$$\mathrm{Im}\, A_{\mathrm{nuc}}(x, t=0) = \int\int \frac{d^2 r dz}{4\pi} \left(\psi_V^* \psi_\gamma\right)_T \sigma_{\mathrm{dip}}^{\mathrm{nuc}}(x, r)$$

where

$$\sigma_{\mathrm{dip}}^{\mathrm{nuc}}(x, r) = 2\int d^2 b' \left\{1 - \exp\left[-\frac{1}{2} T_A(b') \sigma_{\mathrm{dip}}^{\mathrm{proton}}(x, r)\right]\right\}$$

b' is the photon-nuclei impact parameter.

$T_A(b')$ is the nuclear profile function;

- Then, the photoproduction cross section will be

$$\sigma(\gamma A \to VA) \propto |\mathrm{Im}\, A_{nuc}(x, t=0)|^2$$

Theory

Phenomenology

Ultraperipheral Collisions

Peripheral Collisions

Simulations

Summary

Ultraperipheral Collisions

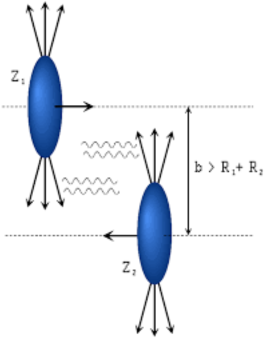

Results for $\sqrt{s} = 7$ TeV in pp collisions

- Comparison of the rapidity distribution for pp collisions with the LHCb data[1]

$$\frac{d\sigma}{dy}(pp \to p \otimes V \otimes p) = \omega \frac{dN_\gamma}{d\omega}\sigma(\gamma p \to Vp) + (y \to -y)$$

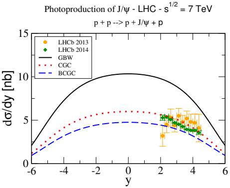

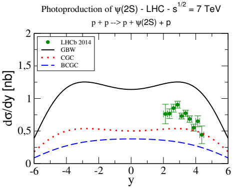

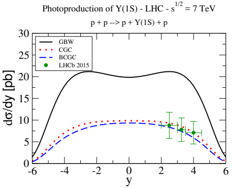

- *GBW* model overestimates the data.

Parametrization: M. Kozlov, A. Shoshi and W. Xiang - JHEP 0710 (2007) 020.

- The other models are consistent with the data of J/ψ and $\Upsilon(1S)$.

M. B. Gay Ducati, F. Kopp, M. V. T. Machado and S. Martins, PRD94, 094023 (2016).

[1] **R. Aaij *et al.*, J. Phys. G40, 045001 (2013); J. Phys. G41, 055002 (2014); JHEP 1509, 084 (2015).**

Results for $\sqrt{s} = 7$ TeV in pp collisions

- Total cross section corrected by acceptance and branching ratio ($BR_{V\to\mu^+\mu^-}$).

$\sqrt{s} = 7$ TeV	GBW	CGC	b-CGC	LHCb
J/ψ [pb]	553.87	316.82	246.29	291$\pm$20 pb
$\psi(2S)$ [pb]	10.80	4.64	2.76	6.5$\pm$1.0 pb
$Y(1S)$ [pb]	22.05	9.25	8.05	9.0$\pm$2.7 pb
$Y(2S)$ [pb]	4.16	1.71	1.59	1.3$\pm$0.85 pb
$Y(3S)$ [pb]	2.07	0.87	0.83	$<$3.4 pb

Results for $\sqrt{s} = 5.02$ TeV in pA collisions

Theory
Phenomenology
Ultraperipheral Collisions
Peripheral Collisions
Simulations
Summary

$$\frac{d\sigma}{dy}(pPb \to p \otimes V \otimes Pb) = \omega(y) N_\gamma^p(\omega(y)) \sigma_V^{\gamma Pb}(\omega(y)) + \omega(-y) N_\gamma^{Pb}(\omega(-y)) \sigma_V^{\gamma p}(\omega(-y))$$

- Comparison of the rapidity distribution for pA collisions with the ALICE data[2]

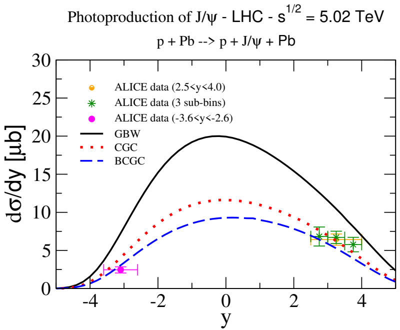

[2] B. B. Abelev et al. Phys. Rev. Lett. 113, (2014) 232504

Results for $\sqrt{s} = 2.76$ TeV in AA collisions

- Comparison of the rapidity distribution for AA collisions with the ALICE data[3]

$$\frac{d\sigma}{dy}(AA \to A \otimes V \otimes A) = \omega \frac{dN(\omega)}{d\omega}\sigma(\gamma A \to VA) + (y \to -y)$$

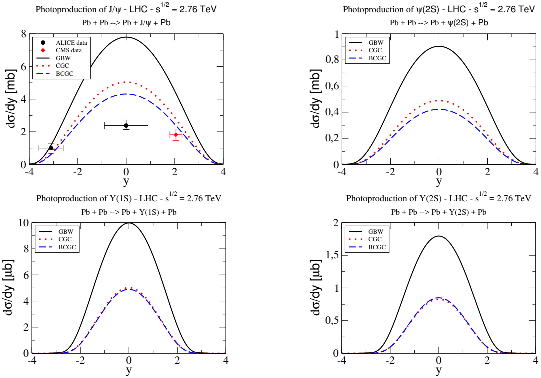

[3] **B. Abelev *et al.*, Phys. Lett. B718, 1273 (2013); E. Abbas *et al.*, Eur. Phys. J. C73, 2617 (2013).**

Peripheral Collisions

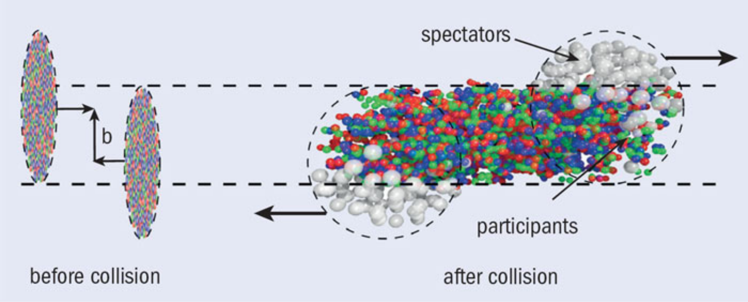

ALICE Measurements - J/ψ

- The Average Rapidity Distribution

$$\left.\frac{d\sigma}{dy}\right|_{2.5<y<4.0} = \frac{1}{\Delta y}\int_{2.5}^{4.0}\frac{d\sigma}{dy}dy$$

- ALICE measurements [4]

$p_T < 0.3$ GeV/c and $\sqrt{s_{NN}} = 2.76$ TeV

Cent.%	$N_{AA}^{J/\psi}$	$N_{AA}^{hJ/\psi}$	$N_{AA}^{\text{excess}J/\psi}$	$d\sigma^{\text{coh}}_{J/\psi}/dy$ [μb]
0-10	339±85±78	406±14±55	<251	<318
10-30	373±87±75	397±10±61	<237	<290
30-50	187±37±15	126±4±15	62±2±5	$73 \pm 44^{+26}_{-27} \pm 10$
50-70	89±13±2	39±2±5	50±14±5	$58\pm16^{+8}_{-10}\pm8$
70-90	59±9±3	8±1±1	51±9±3	$59\pm11^{+7}_{-10}\pm8$

- $N_{AA}^{J/\psi} \rightarrow$ raw number of J/ψ.
- $N_{AA}^{\text{excess}J/\psi} \rightarrow$ excess of J/ψ.
- $N_{AA}^{hJ/\psi} \rightarrow$ raw hadronic number of J/ψ.

[4] ALICE Collaboration, J. Adam et al., Phys. Rev. Lett. 116, 222301, (2016)

Theory

Phenomenology

Ultraperipheral Collisions

Peripheral Collisions

Simulations

Summary

b-Dependence Photon Flux

- For peripheral collisions $\rightarrow N(\omega, b)$ with b-dependence [5],

$$\frac{dN(\omega,b)}{d\omega db^2} = \frac{Z^2\alpha_{qed}}{\pi^2\omega}\left|\int d^2k_T k_T^2 \frac{F(k)}{k^2} J_1(k_T b)\right|^2$$

- Yukawa potential+hard sphere (more realistic for lead) [6],

$$F(k) = \frac{4\pi\rho_0}{Ak^3}\left[\sin(kR_A) - kR_A\cos(kR_A)\right]\left[\frac{1}{1+a^2k^2}\right]$$

- $k^2 = (\omega/\gamma)^2 + k_\perp^2$.
- $\rho_0 = 0.1385$ fm and $a = 0.7$ fm
- A=208 and $R_A = 1.2A^{1/3}$ fm

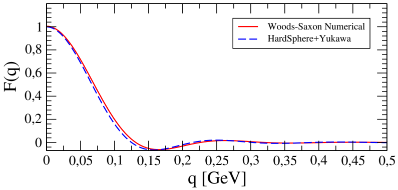

[5] F. Krauss, M. Greiner and G. Soff, Prog. Part. Nucl. Phys. 39, 503, (1997)

[6] K. T. R. Davies and J. R. Nix, Phys. Rev. C14, 1977 (1976).

Comparing the Form Factors

- Centrality classes and related impact parameters range:

Centrality Classes	Glauber Model		ALICE	
	b_{min} (fm)	b_{max} (fm)	b_{min}^{exp} (fm)	b_{max}^{exp} (fm)
30%-50%	7.77	10	8.55	11.04
50%-70%	10	11.87	11.04	13.05
70%-90%	11.87	13.47	13.05	14.96

- Analysis of the different form factors

Photon flux integrated in ω

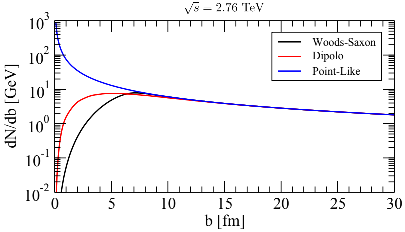

Point Like (used in UPC)

- $F(k^2) = 1$.

Dipole Form Factor

- $F_{\text{dip}}(k^2) = \frac{\Lambda^2}{\Lambda^2 + k^2}$.

Woods-Saxon+Yukawa

- $F_{WSY}(k^2) = \frac{4\pi\rho_0}{Ak^3}\left[\sin(kR_{Pb}) - kR_{Pb}\cos(kR_{Pb})\right]\left[\frac{1}{1+a^2k^2}\right]$.

The Effective Photon Flux

- Considering an effective photon flux [7],

$$\sigma_X = \int \omega \frac{dN^{eff}(\omega)}{d\omega} \sigma_X(\omega)$$

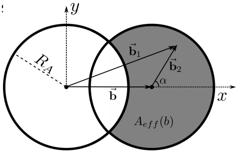

- **Hypothesis:** Only spectators interact coherently with the photon.

- In this scenario, $\frac{dN^{eff}(\omega,b)}{d\omega}$ can be described as [8]

$$N^{eff}(\omega,b) = \frac{1}{A_{eff}(b)} \int N^{usual}(\omega,b_1)\theta(b_1 - R_A)\theta(R_A - b_2)d^2b_2$$

- $A_{eff} = R_A^2\left[\pi - 2\cos^{-1}(b/2R_A)\right] + (b/2)\sqrt{4R_A^2 - b^2}$ and $b_1^2 = b^2 + b_2^2 + 2bb_2\cos(\alpha)$

[7] M. K. Gawenda and A. Szczurek, Phys. Rev. C93, 044912, (2016).

[8] M. B. Gay Ducati and S. Martins, Phys. Rev. D97, 116013, (2018).

The Effective Photonuclear Cross Section

- The forward scattering amplitude is given by

$$\mathrm{Im}\,\mathcal{A}_{nuc}(x,t=0) = \int \frac{d^2r dz}{4\pi} \left(\psi_V^* \psi_\gamma\right)_T \sigma_{\rm dip}^{\rm nucleus}(x,r)$$

where

$$\sigma_{\rm dip}^{\rm nucleus}(x,r) = 2\int d^2b' \left\{1 - \exp\left[-\frac{1}{2} T_A(b')\sigma_{\rm dip}^{\rm proton}(x,r)\right]\right\}$$

- For consistency with the construction of $N^{eff}(\omega, b)$, restrict $\sigma_{dip}^{nucleus}(x,r)$:

$$\sigma_{\rm dip}^{\rm nucleus}(x,r) = 2\int d^2b_2 \Theta(b_1 - R_A) \left\{1 - \exp\left[-\frac{1}{2} T_A(b_2)\sigma_{\rm dip}^{\rm proton}(x,r)\right]\right\}$$

  - $b_1^2 = b^2 + b_2^2 + 2bb_2\cos(\alpha)$.

Our results for dσ/dy

- Essencially, three modification were considered
  - b-dependence.
  - Effective photon flux.
  - Effective Photonuclear cross section.
- Comparing with ALICE data,

Average Rapidity Distribution: $2.5 < y < 4.0$

GBW / CGC	$d\sigma^{\text{theo}}_{J/\psi}/dy$ [μb]	$d\sigma^{\text{exp}}_{J/\psi}/dy$ [μb]
30%-50%	134 / 85	$73\pm44^{+26}_{-27}\pm10$
50%-70%	145 / 91	$58\pm16^{+8}_{-10}\pm8$
70%-90%	138 / 87	$59\pm11^{+7}_{-10}\pm8$

- Better agreement for CGC model.

dσ/dy for different centralities

Theory

Phenomeno-logy

Ultraperipheral Collisions

Peripheral Collisions

Simulations

Summary

- With *b*-dependence

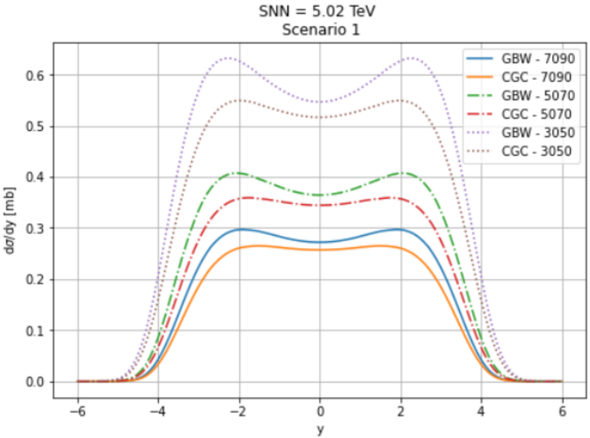

- P. H. Fetter da Luz - 2024

dσ/dy for different centralities

- With *b*-dependence and effective photon flux

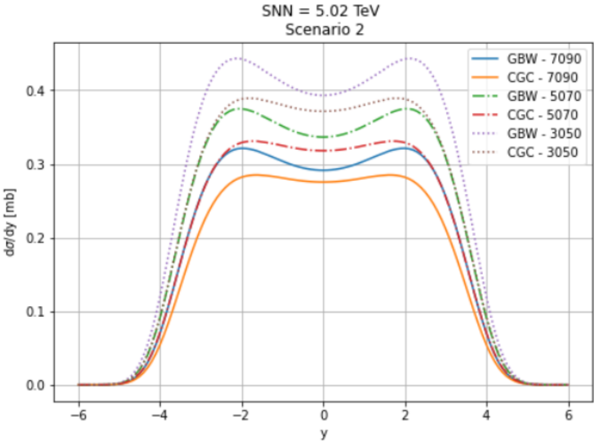

- P. H. Fetter da Luz - 2024

Theory
Phenomenology
Ultraperipheral Collisions
Peripheral Collisions
Simulations
Summary

GFPAE

Theory

Phenomenology

Ultraperipheral Collisions

Peripheral Collisions

Simulations

Summary

dσ/dy for different centralities

- With *b*-dependence, effective photon flux and effective photonuclear cross section

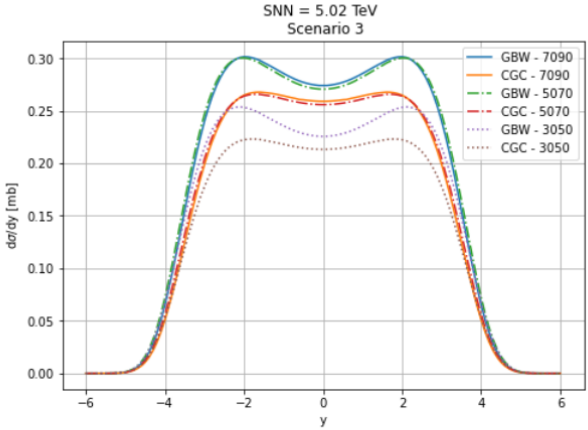

- P. H. Fetter da Luz - 2024

Quark Matter 2022

J/ψ photoproduction in peripheral collisions

- **Transition from ultra-peripheral to peripheral collisions:**
  - Need to account for the geometrical constraints of a given impact parameter
  - Modification of the photon flux / photonuclear cross section

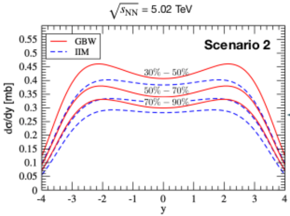

Scenario 1: UPC like
Scenario 2: effective photon flux
Scenario 3: effective photon flux + photonuclear cross section

IIM: Color Glass Condensate approach
GBW: light cone dipole formalism

M. B. Gay Ducati et al., PRD 97 (2018) 11

7

A. Neagu (ALICE Collaboration), "Measurement of charmonium production in Pb-Pb and p-Pb collisions at the LHC with ALICE", PoS, vol. ICHEP2020, p. 557, 2021.

Quark Matter 2022

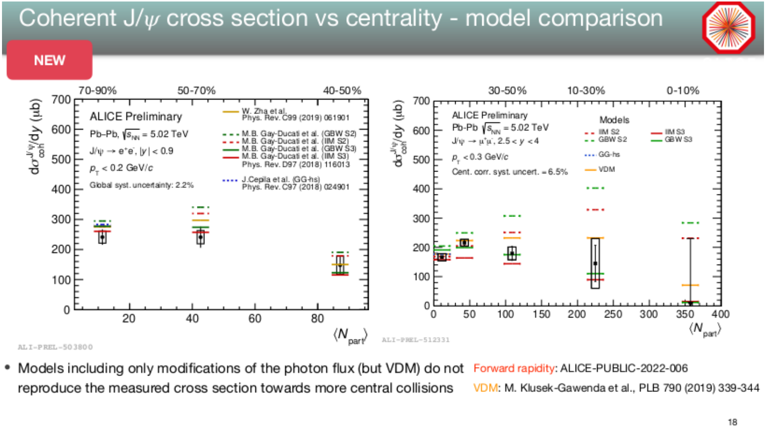

A. Neagu (ALICE Collaboration), "Measurement of charmonium production in Pb-Pb and p-Pb collisions at the LHC with ALICE", PoS, vol. ICHEP2020, p. 557, 2021.

Quark Matter 2023

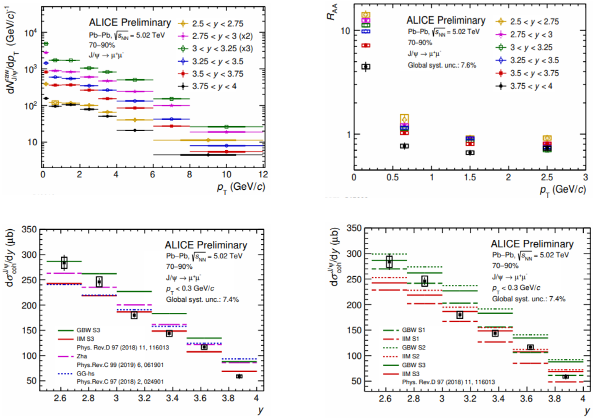

- Significant J/Ψ excess over the hadronic yield observed for $p_T < 0.3$ GeV/c.
- Rise in the R_{AA} indicates that photoproduction occurs at low p_T
- Models can reproduce the magnitude of the cross section, but faces difficulty reproducing the y-dependence

A. Shatat (ALICE Collaboration), "Coherent J/ψ photoproduction and polarization in peripheral Pb–Pb collisions," *EPJ Web Conf.*, vol. 296, p. 07005, 2024, doi: 10.1051/epjconf/202429607005.

NLO study in pQCD

- Scale dependence
- Gluons and quarks contributions (!)
- Nuclear effects

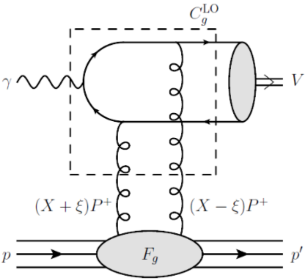

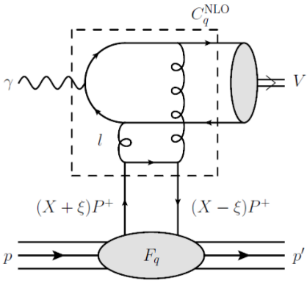

- only gluons GPD's

- Gluons + quarks GPD's

[Ivanov et al., Eur. Phys. J. C 34 (2004) no. 3, 297]

How about data (LHC)?

Figures from C. Flett, PhD thesis [Flett:2021xsl]

NLO study in pQCD: amplitude

K. Eskola et al., arXiv:2203.11613 [hep-ph]

$$\mathcal{M}^{\gamma N \to VN} \propto \langle O_1 \rangle_V^{1/2} \int_{-1}^{1} dx \left[T_g(x,\xi) F^g(x,\xi,t) + T_q(x,\xi) F^{q,S}(x,\xi,t) \right],$$

- $\langle O_1 \rangle_V^{1/2}$ NRQCD element
- T_g *and* T_q hard scattering functions from pQCD[1], scale dependent (μ_F, μ_R)
- F^g *and* $F^{q,S}$ GPDs[2], nonperturbative (μ_F)

$$|\mathcal{M}|^2 = |\mathcal{M}_G^{\mathrm{LO}} + \mathcal{M}_G^{\mathrm{NLO}}|^2 + |\mathcal{M}_Q^{\mathrm{NLO}}|^2 + 2\Big[\mathrm{Re}(\mathcal{M}_G^{\mathrm{LO}} + \mathcal{M}_G^{\mathrm{NLO}})\mathrm{Re}(\mathcal{M}_Q^{\mathrm{NLO}}) + \mathrm{Im}(\mathcal{M}_G^{\mathrm{LO}} + \mathcal{M}_G^{\mathrm{NLO}})\mathrm{Im}(\mathcal{M}_Q^{\mathrm{NLO}})\Big].$$

[1] D. Y. Ivanov, A. Schafer, L. Szymanowski, G. Krasnikov, Eur. Phys. J. C 34 (2004) no. 3, 297 [Erratum: Eur.Phys.J.C 75, 75 (2015)]

Comparison of LO for exclusive J/ψ photoproduction in PbPb

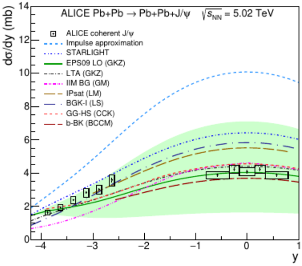

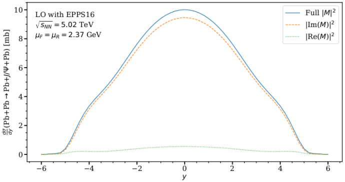

- In pQCD and QCD models
- Linear and non-linear evolution equations.
- The data favour those models

featuring moderate nuclear shadowing.

S. Ragoni, on behalf of the ALICE Collaboration, arXiv:2305.03616v1

- In pQCD
- The $|Re(M)|^2$ in LO is almost irrelevant.

K. Eskola et al., arXiv:2203.11613 [hep-ph]

NLO for exclusive J/ψ photoproduction in PbPb (pQCD) vs colour dipole picture LO (UPC)

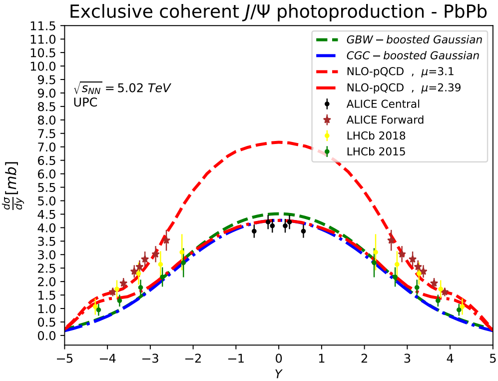

- The data does not support any particular model.
- Our results with dipole picture in LO are shown by the blue solid line and the green dashed line.

K. Eskola et al., arXiv:2203.11613 (pQCD)

The ALICE experiment (Run 4)

- **Physics motivation:**

• J/Ψ photoproduction in ultra-peripheral Pb-Pb collisions reveals important insights into nuclear effects, gluon saturation, and non-perturbative QCD at very low Bjorken-x values.

- **ALICE Experiment:**

• A Large Ion Collider Experiment (ALICE) is designed to study heavy-ions collisions to investigate the properties of quark-gluon plasma.

• Characterizes the QGP by focusing on high-rate data collection (50 kHz and aims to inspect 10 nb^{-1} of Pb–Pb collisions) and enhanced tracking and particle identification systems.

- **New detector:**

•FoCal, the new ALICE detector, will be used to extend heavy quarkonia studies to ultra-peripheral Pb-Pb collisions and lower *x*-values $x < 10^{-6}$.

https://cds.cern.ch/record/2890281

• FoCal's performance in measuring J/Ψ and Ψ' across various collision types was evaluated, confirming its ability to differentiate the particles using simulated data.

The FoCal calorimeter: Performance

- The rapidity coverage of FoCal enables measurements at very low Bjorken-x values, aiding in the investigation of gluon saturation in nuclei.

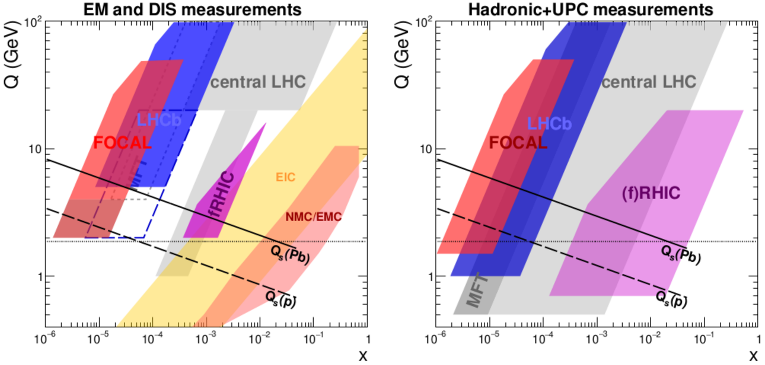

The FoCal *xQ* coverage compared with others detectors.

ALICE Collaboration, *Letter of intent: A forward calorimeter (FoCal) in the ALICE experiment*. CERN, Geneva, Tech. Rep. CERN-LHCC-2020-009, Jun. 2020.

Simulations of J/Ψ and Ψ' production

- We simulated the coherent J/Ψ production in proton-lead, lead-proton and lead-lead collisions;
- It was also simulated the production of Ψ';
- The electromagnetic shower will be absorbed by FoCal, and the data collected will be used for its reconstruction.
- With the kinematics of the simulation the invariant mass is reconstructed;
  - **Simulation:** Employing STARlight to generate J/Ψ and Ψ' events.
  - **Clusterization of Data:** The data are grouped into superclusters and matched with the physical primary particles.
  - **Kinematics:** the data distribution is plotted into histograms.
  - **Invariant Mass:** Reconstruction of the invariant mass using the superclusters data by

$$m = \sqrt{(\vec{p}_{e^-} + \vec{p}_{e^+})^2 - (p_{e^-} + p_{e^+})_x^2 - (p_{e^-} + p_{e^+})_y^2 - (p_{e^-} + p_{e^+})_z^2}.$$

  - **Fit function:** Crystal-ball function used to fit the invariant mass data.

Simulations: Invariant mass for lead-proton collisions

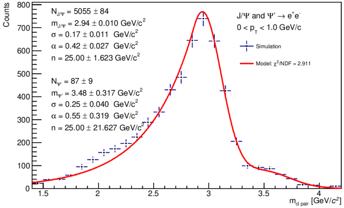

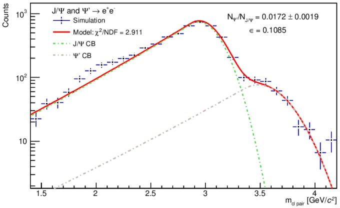

- In lead-proton collisions, as the Pb nucleus moves toward FoCAL, the calorimeter can still distinguish between both particles.

CERN. *Technical Design Report of the ALICE Forward Calorimeter (FoCal)*. CERN, Geneva, 2024. CERN-LHCC-2024-004, ALICE-TDR-022.
LUZ, Paulo Henrique Fetter da. *Use of FoCal to constrain gluons distribution on ALICE*. Master dissertation, Universidade Federal do Rio Grande do Sul, Porto Alegre, Brazil, 2023.

Simulations: Invariant mass for lead-lead collisions

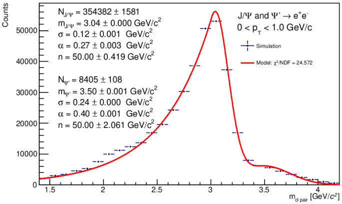

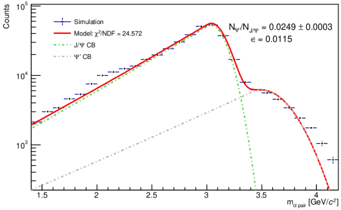

- For Pb-Pb collisions, the two peaks are even more distinct than in proton-lead collisions.

CERN. *Technical Design Report of the ALICE Forward Calorimeter (FoCal)*. CERN, Geneva, 2024. CERN-LHCC-2024-004, ALICE-TDR-022.
LUZ, Paulo Henrique Fetter da. *Use of FoCal to constrain gluons distribution on ALICE*. Master dissertation, Universidade Federal do Rio Grande do Sul, Porto Alegre, Brazil, 2023.

Conclusions and a Look Ahead

- Exclusive quarkonium photoproduction off protons in p-Pb UPC
  - Probe the gluon density at low x
  - Search for gluon saturation effects - quarks role in NLO formulation.
- Photoproduction in peripheral collisions
  - Complements the knowledge on hadroproduction
  - Learning on nuclear medium and quark gluon plasma
- Simulation of the Photoproduction of J/Ψ:
  - Invariant mass reconstruction distinguishes between J/Ψ and Ψ' resonances.
  - Implement the analysis for incoherent production.

$\Longrightarrow$ **Refine theory and implement low-x phenomenology application.**

$\Longrightarrow$ **Experiments (ALICE: FoCal,...) contribution to precise the gluon distribution function.**

People at UFRGS

- **Theory, phenomenology and simulation:**
  - Dr. Maria Beatriz de Leone Gay Ducati
  - Dr. Sony Martins
  - Dr. Fabio Kopp
  - Paulo Henrique Fetter da Luz (Ph.D. student)
  - Eliton Trindade Gomes (Master's student)

- **Instrumentation:**
  - Dr. Cristiano Krug
  - André Valentina (Undergraduate research)
  - Henrique Lacerda (Undergraduate research)
  - Vinicius Mori (Undergraduate research)
  - Pedro Lunardi (Undergraduate research)
  - João Wollmeister (Undergraduate research)

GFPAE

Theory

Phenomenology

Simulations

Summary

Conclusions

Dipole models

- The Golec-Biernat and Wüsthoff (GBW) model [9]:
- Model based on QCD-inspired phenomenology
  - The functional form of the dipole cross-section must have:
- For small r, $\sigma \propto r^2$ (Colour transparency);
- For large r, $\sigma \to constant$ (Ensures saturation).

$$\sigma_{q\bar{q}}^{GBW}(x,r) = \sigma_0[1 - \exp(-r^2 Q_s^2(x)/4)]$$

- $Q_s^2(x) = (x_0/x)^{\lambda_{GBW}}$ is the saturation scale;
- $\sigma_0 = 29.12$ mb, $x_0 = 0.41 \times 10^{-4}$, $\lambda_{GBW} = 0.29$ and $\chi^2/N_{dof} = 3.78$ - old fit - for the extracted data from HERA with charm quark ($Q^2 \leq 10 GeV^2$ and $x \leq 10^{-2}$).

Re-evaluate for this fit[10]

- $\sigma_0 = 27.32$ mb, $x_0 = 0.42 \times 10^{-4}$,

$\lambda_{GBW} = 0.248$ and $\chi^2/N_{dof} = 1.60$.

[9] K. G. Biernat and M. Wüsthoff, Phys. Rev. D59, 014017 (1999); Phys. Rev. D60, 114023 (1999).

[10] K. G. Biernat and S. Sapeta, JHEP 1803 (2018) 102..

Dipole models

- The Iancu, Itakura and Munier (CGC) model [11]:

$$\sigma_{q\bar{q}}^{CGC}(x,r) = \sigma_0 \times \begin{cases} \mathcal{N}_0 \left(\frac{rQ_s}{2}\right)^{2(\gamma_s + (1/\kappa\lambda Y) ln(2/rQ_s))} & : rQ_s \leq 2 \\ 1 - e^{-A ln^2(BrQ_s)} & : rQ_s > 2 \end{cases}$$

- $A = -\frac{\mathcal{N}_0^2 \gamma_0^2}{(1-\mathcal{N}_0)^2 ln(1-\mathcal{N}_0)}$ and $B = \frac{1}{2}(1-\mathcal{N}_0)^{-(1-\mathcal{N}_0)/(\mathcal{N}_0\gamma_s)}$.
- $Y = \ln(1/x)$, $\gamma_s = 0.73$, $\kappa = 9.9$ and $Q_s(x) = (x_0/x)^{\lambda/2}$.
- Free parameters: $\sigma_0 = 27.33$ mb, $\mathcal{N}_0 = 0.7$ and $\lambda = 0.22$.

Features:

For $r \ll 2/Q_s$ (small dipoles), $\mathcal{N}$ obtained from the saddle point approximation to the (LO) BFKL equation;

For $r \gg 2/Q_s$ (large dipoles), functional form of $\mathcal{N}$ obtained from solving the BK equation;

A and B restricted by continuity condition of $\mathcal{N}$ at $rQ_s = 2$

[11] E. Iancu, K. Itakura, and S. Munier, Phys. Lett. B590, 199 (2004).

ALICE Measurements - J/ψ

- The nuclear modification factor (R_{AA}) is given by [12]

$$R_{AA}^{hJ/\psi} = \frac{N_{AA}^{J/\psi}}{BR_{J/\psi \to l^+ l^-} \cdot N_{events} \cdot (A \times \varepsilon)_{AA}^{J/\psi} \cdot \langle T_{AA} \rangle \cdot \sigma_{pp}^{hJ/\psi}}$$

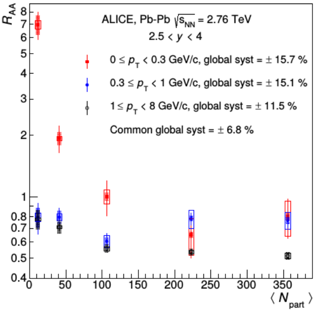

- $N_{AA}^{J/\psi} \to$ raw number of J/ψ
- $BR_{J/\psi \to l^+ l^-} = 5.96\%$
- $N_{events}{}^{a} \simeq 10.6 \times 10^7$
- $(A \times \varepsilon)_{AA}^{J/\psi} \sim 11.31\%$
- $\langle T_{AA} \rangle^{b} = \begin{cases} 3.84\ \mathrm{mb}^{-1}, & 30\% - 50\% \\ 0.954\ \mathrm{mb}^{-1}, & 50\% - 70\% \\ 0.17\ \mathrm{mb}^{-1}, & 70\% - 90\% \end{cases}$
- $\sigma_{pp}^{hJ/\psi} = 0.0514 \mu b$

[a] ALICE Coll., B. Abelev et al., PLB734, 314, (2014)

[b] ALICE Coll., B. Abelev et al., PRC88, 044909,

R_{AA} - Nuclear motification factor

- Black circles: only the b-dependence
  - Best agrees with the data only in the more peripheral region;
- Green losangle: b-dependence + effective photon flux
  - Better results were achieved for the more central classes;
- Blue triangle: All the three modifications was applyed
  - A slight correction in direction to data in relation to last case;

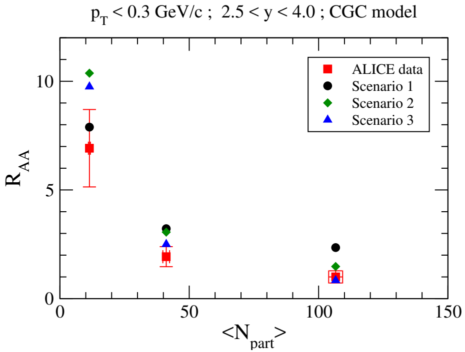

UPC vs Peripheral

The Effective Photon Flow

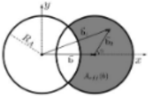

Fig. 1: Scheme of the interaction according to scenario 2.

- From the standard photon flux (N^{usual}) emitted by the projectile nucleus, only the photons that reach the geometric region of the target nucleus will be considered;
- Photons that reach the nuclear superposition region will be discarded (dominated by the strong interaction).

effective photon flow:

$$N^{eff}(\omega, b) = \int N^{usual}(\omega, b_1)\frac{\theta(b_1 - R_A)\theta(R_A - b_2)}{A_{eff}(b)}d^2b_2$$

spectators area:

$$A_{eff}(b) = R_A^2\left[\pi - 2\cos^{-1}\left(\frac{b}{2R_A}\right)\right] + \frac{b}{2}\sqrt{4R_A^2 - b^2}$$

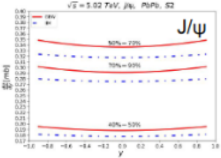

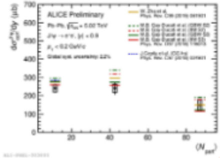

UPC vs Peripheral

The effective photonuclear cross section

- Applying the same geometric constraint on the photonuclear cross section.
  - The dipole-core interaction will be restricted to only the dipole interaction with the part of the core that forms the spectator region

$$\sigma_{\rm dip}^{\rm nucleus}(x,r) = 2\int d^2b_2 \Theta(b_1 - R_A)\left\{1-\exp\left[-\frac{1}{2}T_A(b)\sigma_{\rm dip}^{\rm proton}(x,r)\right]\right\}$$

$$b_1^2 = b^2 + b_2^2 + 2bb_2\cos(\alpha)$$

➢ Effective photon flux and an effective photonuclear cross section

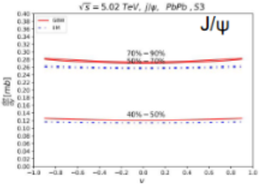

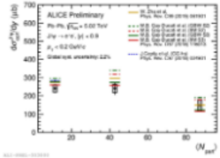

The FoCal calorimeter

The FoCal implementation will be instaled in the **ALICE Experiment** during the **RUN 4** (2027–2029).

CERN. *Technical Design Report of the ALICE Forward Calorimeter (FoCal)*. CERN, Geneva, 2024. CERN-LHCC-2024-004, ALICE-TDR-022.

- **FoCal-E:**
  - Sampling calorimeter with tungsten absorber
  - Pad and pixel layers

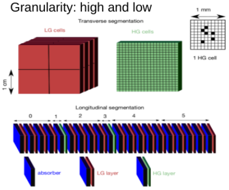

FoCal-E scheme.

- **FoCal-H:**
  - Sampling calorimeter
  - Spaghetti type

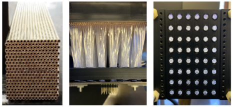

FoCal-H prototype.

Simulations: Invariant mass for proton-lead collisions.

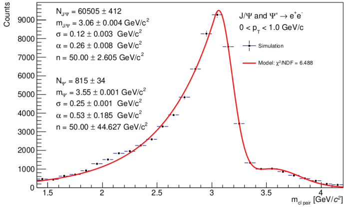

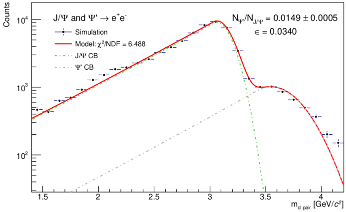

- Invariant mass reconstruction for proton-lead collisions, linear (left) and logarithmic (right) scale. The results show that with FoCal it will be possible to measure and distinguish both J/Ψ and Ψ'.

CERN. *Technical Design Report of the ALICE Forward Calorimeter (FoCal)*. CERN, Geneva, 2024. CERN-LHCC-2024-004, ALICE-TDR-022.
LUZ, Paulo Henrique Fetter da. *Use of FoCal to constrain gluons distribution on ALICE*. Master dissertation, Universidade Federal do Rio Grande do Sul, Porto Alegre, Brazil, 2023.